Medicine®

OBSERVATIONAL STUDY

OPEN

Preoperative CT Predicting Recurrence of Surgically Resected Adenocarcinoma of the Lung

Hyun Jung Koo, MD, PhD, Hai Xu, MD, Chang-Min Choi, MD, PhD, Joon Seon Song, MD, PhD, Hyeong Ryul Kim, MD, PhD, Jung Bok Lee, MD, PhD, and Mi Young Kim, MD, PhD

Abstract: Pathologic lymphovascular invasion (LVI) has been shown to be related to tumor recurrence in lung adenocarcinoma (ADC). We investigated preoperative computed tomography (CT) findings that may be related to pathologic LVI and recurrence of surgically managed stage I–II ADC of the lung.

Consecutive patients (n = 275) with ADC from January 2013 to December 2013 were retrospectively enrolled. Two independent chest radiologists analyzed the CT findings. Clinical, CT (stage, margin, pleural tag, axial location, and peritumoral interstitial thickening), and pathologic findings (stage, % lepidic growth, and LVI) were reviewed. Cox proportional hazard regression analysis was used to estimate the hazard ratios (HRs) for patients with (n = 34) and without (n = 241) recurrence.

The κ index for agreement on the CT findings between radiologists was 0.705 to 0.845. In univariate analysis, % lepidic growth ($P = 0.006$), LVI ($P < 0.001$), size ($P < 0.001$), and staging ($P = 0.011$) differentiated significantly between patients with and without recurrence. Long diameter ($P < 0.001$), mass type ($P < 0.001$), marginal lobulation ($P = 0.020$), central location ($P < 0.001$), and peritumoral interstitial thickening ($P < 0.001$) were significantly related to recurrence on CT. Peritumoral interstitial thickening was positively correlated with tumor size ($P < 0.001$), LVI ($P < 0.001$), N staging ($P = 0.005$), stage ($P < 0.001$), mass type ($P < 0.001$), and recurrence ($P = 0.003$). In multivariate analysis, size (HR, 1.052; 95% CI, 1.022–1.082; $P < 0.001$), central location (HR, 3.152; 1.387–7.166; $P = 0.006$), and LVI (HR, 2.153, 95% CI, 1.038–4.465; $P = 0.039$) were independent predictors of recurrence.

Large, centrally located tumors with LVI tend to recur after surgery. Presence of peritumoral interstitial thickening on CT appears to predict pathologic LVI and recurrence.

(*Medicine* 95(2):e2513)

Abbreviations: ^{18}F-FDG = ^{18}F-fluorodeoxyglucose, AAH = atypical adenomatoid hyperplasia, ADC = adenocarcinoma, AIS = adenocarcinoma in situ, CT = computed tomography, GGO = ground-glass opacity, HR = hazard ratio, HUH = ounsfield unit, LVI = lymphovascular invasion, maxSUV = maximum standardized uptake value, MIA = minimally invasive adenocarcinoma, OR = odds ratio, PET = Positron emission tomography.

INTRODUCTION

The rate of detection of small asymptomatic lung cancers by computed tomography (CT) has increased.[1] Complete surgical resection is the treatment of choice. However, despite early diagnosis and complete resection of nonsmall cell lung cancers (NSCLC), a substantial proportion of patients die of recurrent disease. The 5-year survivals in patients with pathologic stages IA, IB, IIA, and IIB NSCLC according to the 7th edition of the TNM staging are 73%, 58%, 46%, and 36%, respectively.[2,3] Therefore, since tumor recurrence is the most common cause of death and loss of quality of life after surgical resection, it is imperative to predict which patients are susceptible to recurrence and to tailor treatment accordingly, even in operable stages.

Numerous studies have investigated the prognostic impact of patient-related, tumor-related, and treatment-related findings of surgically resectable lung cancer.[3,4] The presence of ground-glass opacities (GGO),[5,6] pathologic lymphovascular invasion (LVI),[7] and ^{18}F-fluorodeoxyglucose (FDG) uptake on positron emission tomography (PET)[8,9] have been introduced as important prognostic factors. However, these studies did not focus on detailed preoperative CT findings, but dealt with clinico-pathologic characteristics of the tumors. Although preoperative TNM staging of lung cancers using CT has been useful for predicting patients' treatment outcomes, tumor recurrence is not adequately predicted by TNM staging alone.

Because adenocarcinoma (ADC) is currently the most common histological type of NSCLC, we aimed to relate pathologic and CT findings in ADC, focusing on peritumoral lymphangitic tumor spread rather than obvious lymph node

Editor: Tuomo Rantanen.
Received: August 10, 2015; revised: December 10, 2015; accepted: December 18, 2015.
From the the Department of Radiology and Research Institute of Radiology (HJK, HX, MYK), Department of Oncology (C-MC), Pulmonary and Critical Care Medicine (C-MC), Department of Pathology (JSS), Thoracic and Cardiovascular Surgery (HRK), and Clinical Epidemiology and Biostatistics (JBL), University of Ulsan College of Medicine, Asan Medical Center, Seoul, Korea; and Department of Radiology, The First Affiliated Hospital of Nanjing Medical University, Nanjing, Jiangsu Province, China (HX).
Correspondence: Mi Young Kim, Department of Radiology and Research Institute of Radiology, University of Ulsan College of Medicine, Asan Medical Center, Olympicro 43 gil 88 Songpa-Gu, Seoul 05505, Korea (e-mail: mimowdr@amc.seoul.kr).
HJK and HX contributed equally to this work.
MYK and HJK had full access to the data in this study and take responsibility for the integrity of the data and the contents of this study. MYK, HJK, and HX contributed to study design, data collection, interpretation, drafting, and review of the manuscript for the content; and final approval of the version to be submitted. C-MC, JSS, and HRK contributed to data acquisition, interpretation, drafting, and review of the manuscript for important intellectual contents; and approval of the final version of the manuscript. JBL and HJK contributed data analysis and interpretation, drafting, and review of the manuscript for important statistical points, and final approval of the manuscript to be submitted.
This work supported by research grant from Korean Association for the Study of Lung Cancer in 2015. The authors have no potential conflicts of interest with any companies/organizations whose products or services may be discussed in this article.
The authors have no conflicts of interest to disclose.

ISSN: 0025-7974
DOI: 10.1097/MD.0000000000002513

metastasis. The correlation between tumor size measured by CT and pathologic features was also examined, especially in tumors with GGO components. The aim of this study was to investigate preoperative CT findings that may related to pathologic LVI and recurrence of surgically managed stage I–II ADC of the lung.

MATERIALS AND METHODS

Patient Characteristics

This retrospective study was approved by the Institutional Review Board (2015-0725), and the requirement for informed consent was waived. We searched the lung cancer registry and electronic medical records at our institution, and the eligibility criteria were as follows: patients with pathologic stage I and II NSCLC who underwent curative operation between January 2013 and December 2013; no separate tumor nodules in the same lobe; and follow-up exceeding 6 months after tumor resection. To analyze tumor size and characteristics on CT and pathology on a per patient basis, patients with separate tumor nodules were excluded. The final pathologic stages were graded based on the 7th edition of the International Association for the Study of Lung Cancer.[10,11] Among the 359 patients who underwent surgical resection, those with prior surgery for lung cancer (n = 14), patients with stage III (n = 49), stage IV (n = 12), separate tumor nodules in the same lobe (n = 7), and insufficient follow-up (n = 2) were excluded (Figure 1).

The data on identified patients (n = 275) (121 males and 154 females) with pathologic stage I and II NSCLC who underwent curative operation were reviewed. Clinical findings including tumor recurrence, CT findings, maximum standardized uptake value (maxSUV) by PET/CT, and pathologic data were reviewed. All patients underwent standardized routine preoperative staging work-up including chest CT, bronchoscopy or CT/fluoroscopic guided-biopsy, and PET/CT scan in real clinical practice. After preoperative evaluation, preoperative staging was performed. Clinical, radiologic, and pathologic findings were compared between patients with and without tumor recurrence.

Surgical Management

Wedge resection (n = 52), lobectomy (n = 209), both wedge resection and lobectomy (n = 12), and bilobectomy (n = 2) were performed in the patients. Intraoperational mediastinal lymph node dissection or sampling of suspected lymph nodes on preoperative evaluation were performed in all patients. The mean interval between preoperative CT exams and curative resection was 12.5 ± 9.2 days.

Pathologic Evaluation

The longest diameter of the tumor (pathologic tumor size) and presence of lepidic growth (%), LVI, and epidermal growth factor receptor were evaluated after pathological subtyping of the ADC by experienced chest pathologists using the surgical specimens. The presence of LVI was assessed by checking for the presence of tumor cells in the lumens of blood vessels or lymphatics. The predominant histologic type of each tumor was also identified. The κ index comparing preoperative T stage on CT and pathologic T stage was obtained.

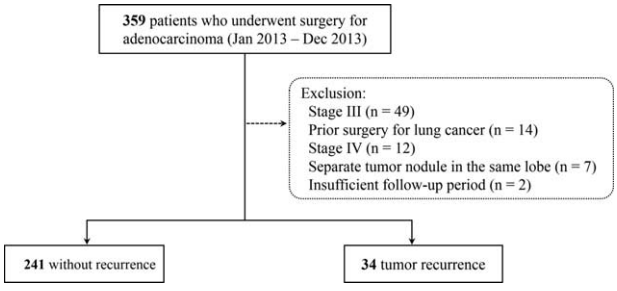

FIGURE 1. Flow diagram of the study patients (n = 275).

Follow-Up for Recurrence

Postoperative follow-up by chest CT were carried out every 3 to 6 months, and PET/CT was done annually. Both local recurrence and distant metastasis were considered to be tumor recurrence. Local recurrence was defined as a tumor appearing at or near the surgical margin or a new lesion occurring in the ipsilateral mediastinum. Patients were periodically monitored for survival until death, at a maximum of 6-month intervals by CT, and annually by PET/CT. Recurrence-free survival was defined as the interval from the date of operation to the date of first documented evidence of recurrence, based on CT scans, PET/CT, and clinical deterioration.

CT Scanning Protocol

Chest CT examinations were performed using 16- or 64-detector CT units, either a SOMATOM Sensation 16 (Siemens Medical Solutions, Erlangen, Germany) or a Lightspeed VCT (General Electric Medical Systems, Milwaukee, WI). Scan parameters were 120 kV, 100 effective mA with dose modulation, 3-/5-mm thickness reconstruction interval without a gap by standard algorithm, and 1-mm thickness with 5-mm gaps by high-frequency algorithm for the 16-detector row scanner. In the 64-detector row scanner, scan parameters were 120 kV, 100 to 400 mA with dose modulation, 2.5-/5-mm thickness reconstruction interval without a gap by lung algorithm, and 1.25-mm thickness with 5-mm gaps by bone algorithm. To obtain contrast enhancement images, 100 mL iopromide 300 (300 mg I/mL Ultravist, Bayer Pharma, Berlin, Germany) was administered intravenously at a rate of 2.5 mL/s using a power injector, and the CT scan was performed after a 50-second delay. All CT scans obtained on axial and coronal images in the settings of the mediastinal (width, 450 Hounsfield unit [HU]; level, 50 HU), lung (width, 1500 HU; level, −700 HU) and bone (width, 1000 HU; level 200 HU) windows were reviewed on the picture archiving and communication system.

CT Evaluation

The 2 independent board-certified radiologists were blind to the clinical data except for the fact that the patient had an ADC treated by surgery. Final conclusions regarding the CT examination findings were reached in consensus. Tumor measurements were obtained on the basis of review of transverse images of the tumor. Main tumors were measured for size, defined as the length of the long diameter in millimeters and divided into 2 types, comprising nodule-type lesions (defined as those $\leq$30 mm) and masses (>30 mm). A lobulated margin was defined as the presence of at least 3 undulations with a height of more than 2 mm, and a spiculated margin was defined as the presence of linear strands at least 2 mm thick extending from the nodule or mass margin into the lung parenchyma.[12] The presence of peritumoral interstitial thickening adjacent to or surrounding the lung cancer, which may suggest a localized form of lymphangitic tumor spread, was assessed (Figures 2 and 3). The concept of peritumoral interstitial thickening was derived from the finding that localized lymphangitic carcinomatosis usually occurs in the peribronchovascular, centrilobular

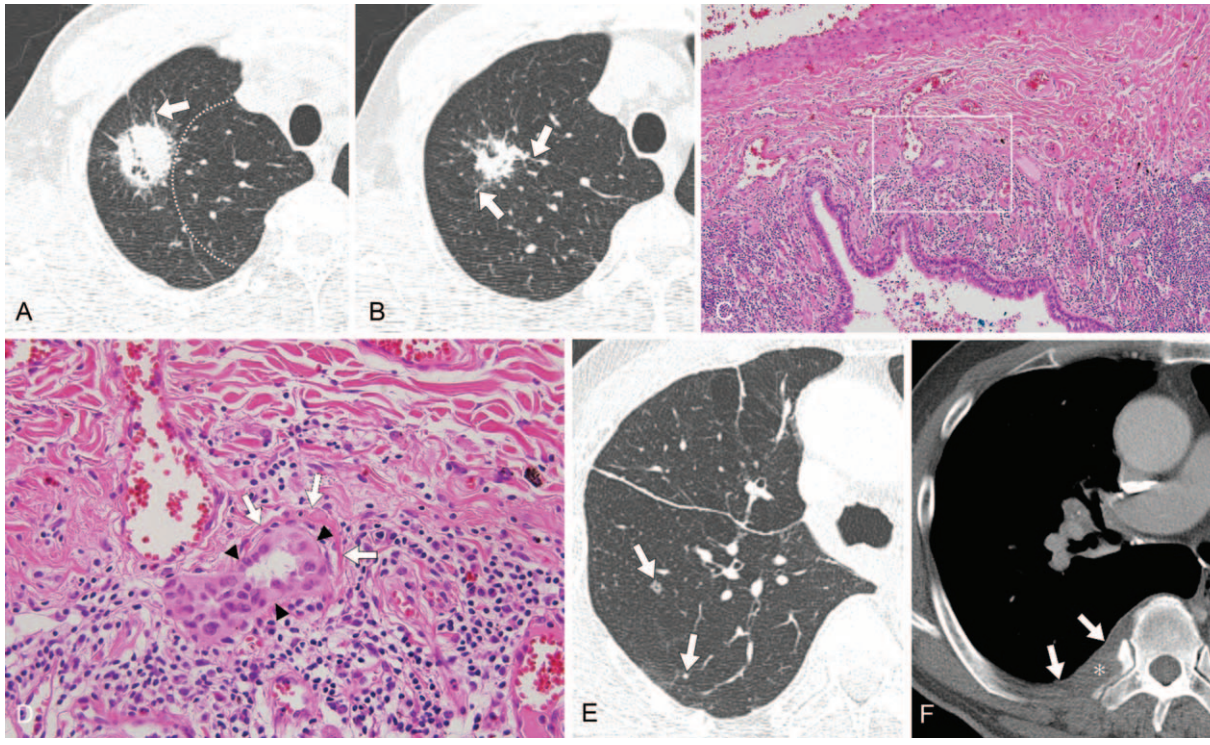

FIGURE 2. CT image obtained in a 69-year-old man with adenocarcinoma of the lung with recurrence in lung and bone after right upper lobectomy. (A, B) Thin-section axial CT lung images (1-mm thickness) obtained at the prevascular level. Images show a 32-mm sized peripheral lung mass (dotted lines, central imaginary line) with spiculated margin, peritumoral interstitial thickening (arrows), sun burst shape, in the right upper lobe, shown to be adenocarcinoma (acinar type). Right upper lobectomy was performed. (C) On histopathologic analysis, the tumor has extensive lymphovascular invasion (hematoxylin–eosin stain, original magnification ×100). The white box indicates the region in figure (D). (D) High power field image showing tumor cells (black arrowheads) invading a blood vessel (white arrows) (hematoxylin–eosin stain, original magnification ×400). The tumor was classified as pathologic T2a N1 M0. (E, F) Follow-up, thin-section axial CT lung image (1-mm thickness) obtained 15 mo after surgery, and axial CT bone image (5-mm thickness) obtained at the levels of the carina and right pulmonary artery, respectively. Images show newly developed small nodules (arrows) in the right lower lobe (E) and a soft tissue lesion involving the pleura (arrows) and causing destruction of the right 7th rib (asterisk) (F). CT = computed tomography.

interstitium, and along the interlobular septa or in subpleural locations with a perilymphatic distribution. The presence of pleural tag, axial location (central or peripheral to a central imaginary line of the lung; Figure 2) and the characteristics (GGO, part solid, and solid) of the tumors were also evaluated.

PET/CT Scanning Protocol

The FDG PET/CTs (Discovery PET/CT 690; GE Health Care Milwaukee, WI) were obtained using a cut-off value of 2.5 times the maxSUV. The maxSUV was calculated by considering the lean body mass-based standardized uptake value. Fifty minutes prior to PET/CT, ^{18}F-FDG (5.2 MBq/kg body weight) was administered intravenously to each patient, who had fasted for more than 6 h. Three-dimensional PET was acquired and CT attenuation corrections for deriving attenuation maps were performed. The mean interval between CT and PET/CT studies was 6 (range, 0–37) days. On the FDG PET/CT images, the highest maxSUV value of the cancer in the largest region of interest not containing any tumor margin or extratumoral component was obtained.

Statistical Analysis

Univariate and multivariate Cox proportional hazard regressions were used to estimate hazard ratios (HRs) for tumor recurrence according to the clinical, pathologic, and preoperative CT findings. After statistically significant pathologic and radiological factors had been selected, the HRs of the prognostic factors for tumor recurrence were obtained by multivariate Cox regression analysis with backward conditional selection. The interobserver agreement was obtained to evaluate the consistency between the CT findings of the 2 radiologists with respect to solidity, margin, peritumoral interstitial thickening, and pleural tag. Pathologic T stage was compared to CT stage by calculating the κ index. Because of collinearity between pathologic tumor size and CT tumor size, the correlations between the 2 parameters and tumor recurrence were evaluated using simple correlation analysis. The association between the presence of peritumoral interstitial thickening and other parameters including pathologic LVI were examined using the Mann–Whitney *U* test and Pearson chi-squared test. Recurrence-free survival was obtained by the Kaplan–Meier method, and *P* values generated by the Tarone–Ware method are shown. All statistical analyses were performed (JBL, with 14 years of experience in statistical analysis) using commercial software (SPSS version 18.0, SPSS, Inc., Chicago, IL).

RESULTS

Patient Clinicopathologic Characteristics

The results of univariate Cox proportional hazard analysis for clinical and pathological predictive factors for tumor

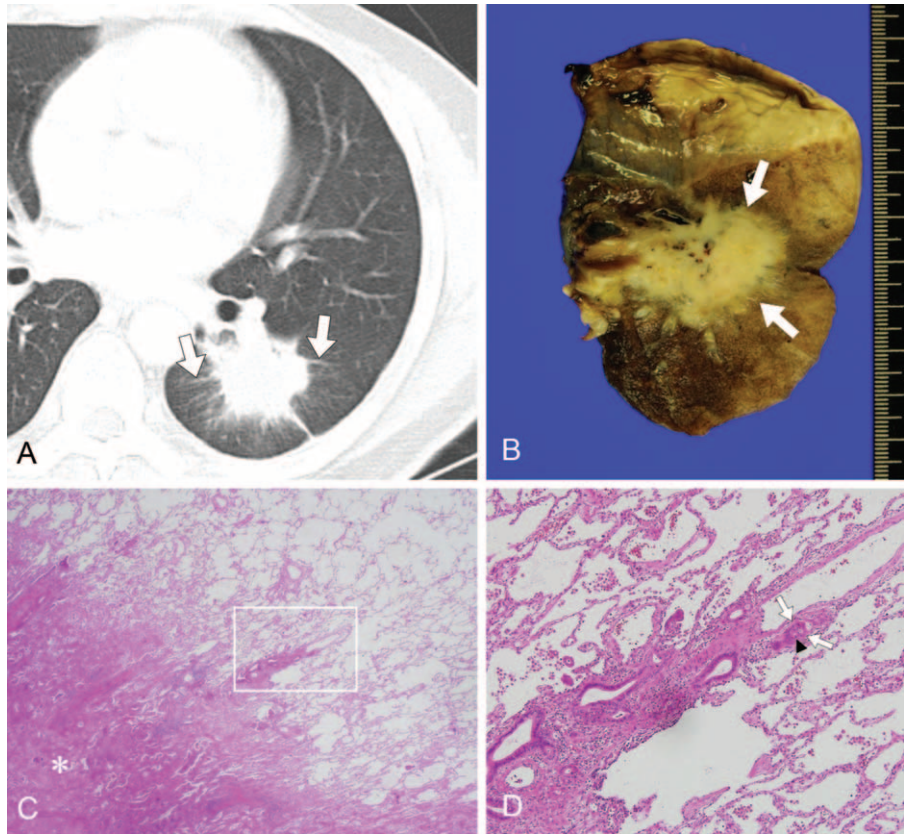

FIGURE 3. CT image obtained in a 50-year-old man with adenocarcinoma of the lung with recurrence in lung and lymph nodes after left lower lobectomy. (A) Thin-section axial CT lung image (1-mm thickness) obtained at the level of the left lower lobar bronchus. Image shows a centrally located 43-mm tumor with peritumoral interstitial thickening (arrows) in the left lower lobe, shown to be a mucinous adenocarcinoma. Left lower lobectomy was performed. (B) The gross specimen is a yellowish mass (arrows) confined to the lung without pleural invasion but with pleural retraction. (C) On histopathologic analysis, the tumor has a spiculated margin with partly lepidic pattern (hematoxylin–eosin stain, original magnification ×12.5). The white box indicates the region shown in (D). (D) The interstitium of the lung is widened and thickened by tumor invasion (black arrowheads) and tumor cells are also evident in the lymphatics (white arrows) (hematoxylin–eosin stain, original magnification ×400). The tumor was classified as pathologic T2a N1 M0. Lymph node metastasis (4R) occurred after 15 mo despite surgery, and lung metastasis followed 20 mo after tumor resection (not shown). CT = computed tomography.

recurrence are shown in Table 1. Tumor recurrence was observed in 34 (2.4%) of the 275 patients, with local recurrence in 6 patients and distant metastasis in 28 patients. The median time from operation to local recurrence or distant metastasis was 13.6 months (range, 0.8–25.9), and the overall follow-up period was 21.0 months (range, 6.0–30.5). There were no significant differences in age, gender, and smoking habit between patients without tumor recurrence (n = 241) and those with recurrence (n = 34). Pathologically, % lepidic growth (HR, 0.952; 95% CI, 0.919–0.986; $P = 0.006$), presence of LVI (HR, 3.875; 95% CI, 1.913–7.851; $P < 0.001$), pathologic tumor size (HR, 1.059; 95% CI, 1.035–1.084; $P < 0.001$), and pathologic stage including T stage ($P < 0.001$) were significantly different in the patients with and without tumor recurrence.

Numbers of metastatic lymph nodes were counted, and the mean number of metastatic lymph nodes was 0.2 ± 0.7. Pathologic N stage and number of metastatic lymph nodes were not statistically significant parameters for predicting tumor recurrence. All solitary precancerous and cancerous lesions including adenocarcinoma in situ (AIS), atypical adenomatoid hyperplasia (AAH), and minimally invasive adenocarcinoma (MIA) were found in the patients without recurrence. Because only 1 primary lung cancer was selected for measurement on CT, any co-existing AAH, AIS, or MIA in the resected specimen was not counted. The surgical methods were not significantly different in the 2 groups ($P > 0.05$).

CT Evaluation

There was excellent to good inter-reader agreement (κ coefficient range, 0.705–0.845). The results of univariate analysis for possible predictive factors for tumor recurrence by CT are shown in Table 2. Tumor size (HR, 1.078; 95% CI, 1.051–1.106; $P < 0.001$), mass type (HR, 4.233; 95% CI, 2.154–8.321; $P < 0.001$), marginal lobulation (HR, 2.238; 95% CI, 1.136–4.411; $P = 0.020$), pleural tag (HR, 3.574; 95% CI, 1.090–11.720; $P = 0.036$), central location (HR, 4.187; 95% CI, 1.948–9.001; $P < 0.001$), solid component (HR, 8.752; 95% CI, 2.095–36.562; $P = 0.003$), and presence of peritumoral interstitial thickening (HR, 5.678, 95% CI, 2.315–13.923, $P < 0.001$) were statistically significant predictors of tumor recurrence in univariate analysis. The maxSUV of

TABLE 1. Univariate Cox Proportional Hazard Analysis of Clinical and Pathologic Findings for Adenocarcinoma in Patients With and Without Recurrence

Parameter	No Recurrence (N = 241)	Recurrence (N = 34)	HR (95% CI)	*P* Value
Age, y	61.2 ± 9.2	61.4 ± 9.1	1.015 (0.977–1.056)	0.438
Gender, M:F	107:134	14:20	1.012 (0.511–2.006)	0.972
Smoking, pack year				0.422
Non-/ex-smokers	8 (3.3)/78 (32.4)	0 (0)/14 (41.2)	1†	
Current smoker	155 (64.3)	20 (58.8)	1.324 (0.668–2.623)	
Pack year	10.1 ± 18.9	8.0 ± 13.2	0.997 (0.977–1.018)	0.772
Pathology				
% Lepidic growth	19.9 ± 28.7	4.3 ± 9.1	0.952 (0.919–0.986)	0.006
Lymphovascular invasion	31 (12.9)	13 (38.0)	3.875 (1.913–7.851)	<0.001
Pathologic tumor size, mm	23.4 ± 11.4	31.2 ± 14.0	1.059 (1.035–1.084)	<0.001
EGFR	174 (72.2)	28 (82.4)	1.694 (0.699–4.101)	0.243
Stage I:II	214:27 (11.2)	25:9 (26.4)	2.705 (1.259–5.809)	0.011
Pathology T stage				
T1a	101 (41.9)	6 (17.6)	1†	<0.001
T1b	89 (36.9)	14 (41.2)	2.967 (1.134–7.761)	0.027
T2a	43 (17.8)	10 (29.4)	4.903 (1.776–13.533)	0.002
T2b	8 (3.3)	4 (11.8)	17.981 (4.880–66.252)	<0.001
Nodule (>30 mm)	190 (78.8)	20 (58.8)	1†	
Mass (≤30 mm)	51 (21.2)	14 (41.2)	3.271 (1.645–6.506)	0.001
Pathology N stage				
N0	221 (91.7)	27 (79.4)	1†	
N1	20 (8.3)	7 (20.6)	2.240 (0.972–5.106)	0.058
No. of metastatic LNs	0.17 ± 0.69	0.21 ± 0.41	1.046 (0.661–1.654)	0.849
Histologic subtype				
Papillary	133 (55.2)	21 (61.8)		
Micropapillary	0 (0.0)	1 (2.9)		
Acina	51 (21.2)	10 (29.4)		
Lepidic	41 (17.0)	0 (0.0)		
Solid	3 (1.2)	1 (2.9)		
Mucinous	12 (5.0)	1 (2.9)		
Not defined	1 (0.4)			
Micropapillary or solid predominant*	3 (1.2)	2 (5.9)	1.672 (0.397–7.044)	0.483
AAH/AIS/MIA	10 (4.1)	0 (0)		
Operation method				
Wedge resection	44 (18.3)	8 (23.5)	1†	0.593
Lobectomy	187 (77.6)	22 (64.7)	0.776 (0.090–6.692)	0.818
Both wedge resection and lobectomy OR bilobectomy	10 (4.1)	4 (11.8)	1.268 (0.171–9.399)	0.816
CT to operation, d	12.7 ± 9.1	10.9 ± 9.6		
F/U period, d	600.5 ± 146.8	640.7 ± 104.8		

Means ± standard deviations. Unless otherwise indicated, data are number of patients, with percentage in parentheses.

AAH = atypical adenomatoid hyperplasia, AIS = adenocarcinoma in situ, CI = confidence interval, CT = computed tomography, EGFR = epidermal growth factor receptor, HR = hazard ratio, LN = lymph node, MIA = minimally invasive adenocarcinoma.

* The reference standard for analysis was the sum of the patients with other findings.

† Reference standard.

the tumors also differed between the 2 groups (HR, 1.127; 95% CI, 1.037–1.225; $P = 0.005$).

The correlation between T stage assessed by pathologic and CT findings was good ($\kappa = 0.658$, $P < 0.001$). However, for the tumors that presented as GGO or part-solid lesions (n = 81, 29.5%), the mean size on pathology (17.7 ± 9.2 mm) was smaller than on CT (19.5 ± 9.2 mm). The correlation between T stage based on pathologic versus CT findings for GGO or part-solid lesions was moderate ($\kappa = 0.508$, $P < 0.001$) and less than for solid lesions ($\kappa = 0.698$, $P < 0.001$). Moreover, tumor size on CT ($r = 0.303$, $P < 0.001$) was more closely correlated with tumor recurrence than pathologic tumor size ($r = 0.215$, $P < 0.001$).

Peritumoral Interstitial Thickening

Peritumoral interstitial thickening on CT was positively correlated with tumor size ($P < 0.001$). However, % lepidic

TABLE 2. Univariate Cox Proportional Hazard Analysis of CT Findings for Adenocarcinoma in Patients With and Without Recurrence

Parameter	No Recurrence (N = 241)	Recurrence (N = 34)	HR (95% CI)	*P* Value
Tumor size on CT, mm	22.9 ± 10.1	32.9 ± 12.9	1.078 (1.051–1.106)	<0.001
Type				
Mass (>30 mm)	50 (20.7)	17 (50)	4.233 (2.154–8.321)	<0.001
Nodule (≤30 mm)	191 (79.3)	17 (50)		
Margin* (κ = 0.845)				
Lobulated	83 (34.4)	19 (55.9)	2.238 (1.136–4.411)	0.020
Spiculated	51 (21.2)	7 (20.6)	1.228 (0.532–2.830)	0.630
Peripheral GGO	102 (42.3)	8 (23.5)	0.049 (0.000–5.232)	0.669
Circumscribed	5 (2.8)	0 (0.0)	0.372 (0.168–0.823)	0.015
Pleural tag	183 (75.9)	31 (91.2)	3.574 (1.090–11.720)	0.036
Axial location (κ = 0.797)				
Central	223 (92.5)	25 (70.6)	4.187 (1.948–9.001)	<0.001
Peripheral	18 (7.5)	9 (26.5)	1†	
Character (κ = 0.705)				
GGO/part solid	12 (5.0)/67 (27.8)	0 (0)/2 (5.9)	1†	0.003
Solid	162 (67.2)	32 (94.1)	8.752 (2.095–36.562)	
Peritumoral interstitial thickening (κ = 0.820)	11 (4.5)	6 (17.6)	5.678 (2.315–13.923)	<0.001
MaxSUV on PET/CT	3.4 ± 3.5	5.1 ± 4.0	1.127 (1.037–1.225)	0.005

Means ± standard deviations. Unless otherwise indicated, data are number of patients, with percentages in parentheses. κ index indicates inter-reader agreement.

CI = confidence interval, CT = computed tomography, GGO = ground-glass opacity, HR = hazard ratio, MaxSUV = maximum standardized uptake value, PET = positron emission tomography.

* The reference standard for each analysis was the sum of the patients with other findings.

† Reference standard.

growth was lower in the patients with peritumoral interstitial thickening than in those without it ($P = 0.04$). The odds ratios (OR) for pathologic LVI (OR, 5.481, 95% CI, 1.986–15.131, $P < 0.001$), pathologic N staging (OR, 4.470; 95% CI, 1.442–13.851; $P = 0.005$), stage (OR, 7.302; 95% CI, 2.607–20.452; $P < 0.001$), mass type (OR, 8.858; 95% CI, 2.993–26.215; $P < 0.001$), and tumor recurrence (OR, 4.481; 95% CI, 1.538–13.053; $P = 0.003$) were higher in patients with peritumoral interstitial thickening (Table 3). An example of a tumor with peritumoral interstitial thickening on CT that correlated with pathological LVI is shown in Figure 3.

Predictors for Tumor Recurrence

In a multivariate Cox proportional hazard analysis of CT parameters, tumor size on CT (HR, 1.061; 95% CI, 1.032–1.091; $P < 0.001$) and central location (HR, 2.835; 95% CI, 1.200–6.701; $P = 0.018$) were significant predictors of tumor recurrence (Table 4). The presence of peritumoral interstitial thickening had a marginally significant relation to tumor recurrence (HR, 2.581; 95% CI, 0.999–6.669; $P = 0.50$). Based on both CT and pathology parameters, tumor size on CT (HR, 1.052; 95% CI, 1.022–1.082; $P < 0.001$), axial location of tumor (HR, 3.152; 1.387–7.166; $P = 0.006$) and pathologic LVI (HR, 2.153; 95% CI, 1.038–4.465; $P = 0.039$) were independent predictors of recurrence. Because the correlations for staging, namely overall stage and T and N stage, were not higher than those for these 3 predictors above, a sub-group analysis for stage I versus II was not performed. Recurrence-free survival curves for the predictability of tumor recurrence using peritumoral interstitial thickening, pathologic LVI, axial location, and tumor size (30-mm as a cut-off) are shown in Figure 4. All *P* values obtained were <0.001.

DISCUSSION

This study examines the associations between tumor recurrence and the clinical, pathologic, and preoperative CT findings, including peritumoral interstitial thickening, in resectable ADC. A previous study demonstrated application of the recurrence risk-scoring model for stage I ADC of the lung in surgical oncology.[4] The results of our study agree with those of that study. In sum, recurrent tumors after resection of ADC tend to be larger, of higher T stage and N stage, and have pathologic LVI. However, in the previous study, detailed CT findings were not well-described with respect to radiologists' stance. Preoperative CT findings other than tumor size, such as tumor character, margin, pleural tag, peritumoral interstitial thickening, and axial location of the tumor as assessed by expert chests radiologists, may be related to tumor recurrence. In view of the recurrence rate in the high-risk group, adjuvant chemotherapy could play a role. For example, even in patients with resectable lung cancer, patients with tumors ≥40 mm had a survival advantage when they received adjuvant chemotherapy.[13] Further investigations should be performed to identify candidates for close follow-up and adjuvant chemotherapy.

ADC is a heterogeneous entity with diverse clinical, radiological, and pathological features.[14] Initially, ADC of the lung develops as a GGO and the solid portion tends to increase over time.[15,16] In the present study, there were no GGO-type tumors in the tumor recurrence group, apart from 2

TABLE 3. Association Between Radiologic and Pathologic Findings and Presence of Peritumoral Interstitial Thickening

Parameter	No PIT (N = 258)	PIT (N = 17)	OR (95% CI)	*P* Value
Tumor size on CT, mm	23.1 ± 10.1	39.5 ± 12.5		<0.001*
Pathologic tumor size, mm	23.4 ± 11.2	39.2 ± 14.3		<0.001*
% Lepidic growth	18.0 ± 27.6	9.9 ± 16.9		0.04*
Lymphovascular invasion	36 (14.1)	8 (47.1)	5.481 (1.986–15.131)	<0.001†
Pathologic N stage (N0:N1)	236:22	12:5	4.470 (1.442–13.851)	0.005†
Stage I:II	230:28	9:8	7.302 (2.607–20.452)	<0.001†
Mass (>3 cm)	55 (21.3)	12 (70.6)	8.858 (2.993–26.215)	<0.001†
Tumor recurrence	28 (10.9)	6 (35.3)	4.481 (1.538–13.053)	0.003†

Means ± standard deviations. Unless otherwise indicated, data are number of patients, with percentages in parentheses.
CI = confidence interval, OR = odds ratio, PIT = peritumoral interstitial thickening.
* Mann–Whitney *U* test.
† Pearson chi-squared test.

part-solid GGO lesions. Pre- or early malignant tumors such as AAH, AIS, or MIA with a GGO component were mostly lepidic subtypes, and so rarely recurred.

The correlations of tumor size measured on CT and pathologic specimens with tumor recurrence are also of questionable value. Although pathologic T stage is the gold standard for tumor staging, the true diameter of the tumor may not be obtained from a shrunken or partially divided tumor specimen, especially 1 with a lepidic component. In this study, in tumors that presented as GGO or part-solid lesions (n = 81), mean size based on pathology was less than that based on CT. Moreover, tumor size on CT was more closely correlated with tumor recurrence than was pathologic tumor size, and this suggests that preoperative CT should be used as a source of accurate parameters for predicting tumor recurrence.

Predominantly lobulated ADC displayed more papillary and micropapillary growth than did spiculated and smooth ADC.[17] To date, lobulated margins are thought to be the only reliable CT feature that allow prediction of malignancy because they point to uneven growth rates with foci of malignant cells at the periphery of the tumor.[12,18] Previous studies have demonstrated the prognostic value of LVI on pathology.[4] We believe that intrapulmonary lymphangitic tumor spread is important, as well as obvious hilar or mediastinal lymph node metastasis.[11] Centrally located lesions also had a tendency toward axial interstitial thickening and lymphangitic carcinomatosis in a previous study.[19]

Furthermore, radiologic and pathologic findings such as CT and pathologic tumor size, pathologic LVI, mass type, and recurrence were closely correlated with the presence of peritumoral interstitial thickening in this study. Radiologist can therefore expect that patients with large tumors, lobulated margin, pleural tag, central location, solid rather than GGO or part-solid GGO characteristics, and presence of peritumoral interstitial thickening on preoperative CT images will have tendency to recur despite being operable.

A diagnostic and therapeutic plan for lung cancer has been developed in our outpatient clinic consisting of a multidisciplinary approach involving radiologists, pulmonologists, oncologists, radiation oncologists, and thoracic surgeons. Radiologists can contribute to the development of effective treatment plans by suggesting the possibility of recurrence on the basis of initial chest CT. Alertness on the part of radiologists about localized lymphangitic tumor spread in stage I, II ADC is important; likewise about widespread lymphangitic carcinomatosis. Our study might also provide the basis for a surgical decision to employ limited surgical resection without lymph node dissection in pulmonary ADC presenting as pure or part solid GGO nodules.[20]

This study has several limitations. It is a retrospective study, performed in a single tertiary center. Hence, there was a selection bias toward recurrence. Tumors with mixed GGOs are most common in East Asia so there may also be an ethnic bias. The diversity of the CT findings prevented them from being

TABLE 4. Multivariate Cox Proportional Hazard Analysis for Estimating Prognostic Factors on Preoperative CT and Pathology for Recurrence of Adenocarcinoma

	Parameter	HR	95% CI	*P* Value
CT only	Tumor size on CT	1.061	1.032–1.091	<0.001
	Central location	2.835	1.200–6.701	0.018
	Peritumoral interstitial thickening	2.581	0.999–6.669	0.050
CT and pathologic parameters	Tumor size on CT	1.052	1.022–1.082	<0.001
	Central location	3.152	1.387–7.166	0.006
	Lymphovascular invasion	2.153	1.038–4.465	0.039
	% Lepidic portion	0.968	0.933–1.004	0.082

CI = confidence interval, CT = computed tomography, HR = hazard ratio.

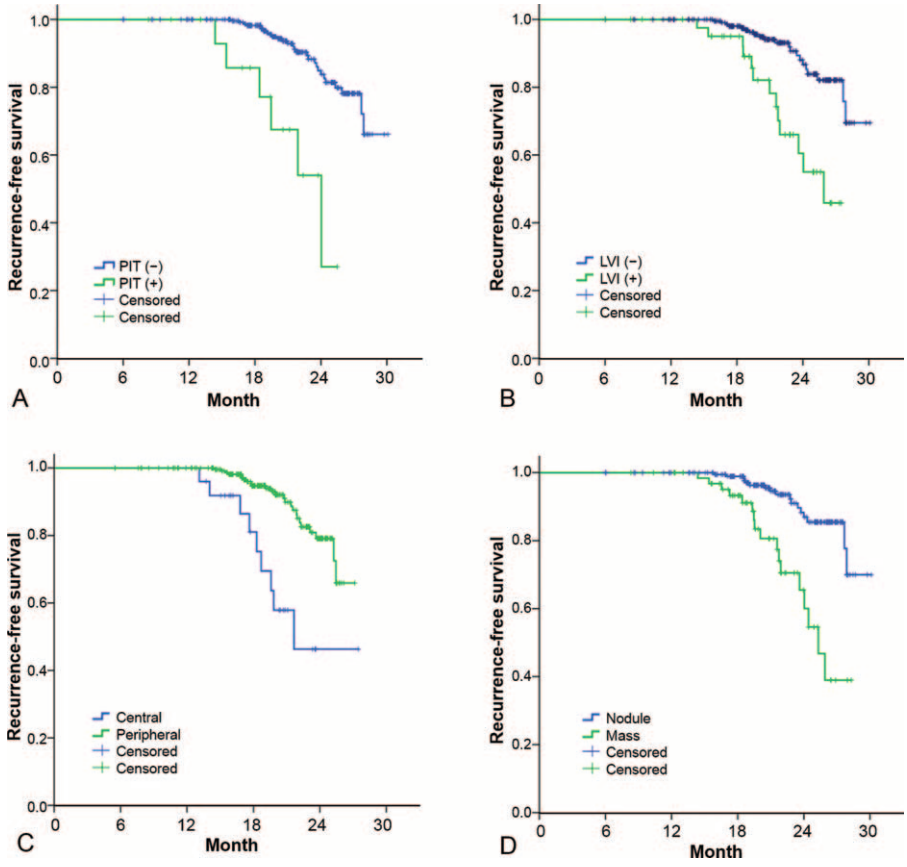

FIGURE 4. Graphs comparing the predictability of tumor recurrence in patients with and without recurrence on the basis of (A) peritumoral interstitial thickening (PIT) on CT (B) pathologic lymphovascular invasion (LVI) (C) axial location (central vs peripheral) and (D) nodule or mass type of the main tumor. Graphs were drawn with data from all patients with no missing data. All *P* values were <0.001. (+), positive, (−), negative, CT = computed tomography.

classified into our usual broad spectrum of ADCs. Second, in our cohort of 275 patients, the number of patients in the recurrence group was smaller than in the no recurrence group. The absolute recurrence rate was 12.4%, despite including stage II, during a median follow-up of 21.0 months, which may have been inadequate. However, it may include the majority of the tumor recurrences, because the median time from operation to recurrence was 13.6 months. Third, the number of patients who had peritumoral interstitial thickening was small, even though the frequency of this finding differed significantly between patients with and without tumor recurrence. Also, there may be a subjective element in the image findings especially in cases of peritumoral interstitial thickening, while these tumors may be combined with pneumonia which could mimic the finding. However, our results, which were assessed by 2-board-certified chest radiologists familiar with the interpretation of lymphangitic carcinomatosis of the lung on chest CT, are useful and practical. This cohort could be used as providing baseline visual assessment data for comparison with a forthcoming computerized texture analysis of lung cancer using CT.[21,22]

CONCLUSION

In conclusion, tumors of large size with solid components, mass-type tumors, lobulated margins, central location of the lesion, and presence of peritumoral interstitial thickening are significant predictor of recurrence compared with tumors of small size with GGO components, nodule-type tumors, no distinct lobulation, peripheral location, and absence of peritumoral interstitial thickening on preoperative CT. Peritumoral interstitial thickening on preoperative CT appears to predict pathologic LVI and recurrence.

ACKNOWLEDGMENT

We thank Dr Julian D. Gross for help with the English language.

REFERENCES

1. Swensen SJ, Jett JR, Hartman TE, et al. CT screening for lung cancer: five-year prospective experience. *Radiology.* 2005;235:259–265.
2. Goldstraw P, Crowley J, Chansky K, et al. The IASLC Lung Cancer Staging Project: proposals for the revision of the TNM stage groupings in the forthcoming (seventh) edition of the TNM Classification of malignant tumours. *J Thorac Oncol.* 2007;2:706–714.
3. Chansky K, Sculier JP, Crowley JJ, et al. The International Association for the Study of Lung Cancer Staging Project: prognostic factors and pathologic TNM stage in surgically managed non-small cell lung cancer. *J Thorac Oncol.* 2009;4:792–801.

4. Yang HC, Kim HR, Jheon S, et al. Recurrence risk-scoring model for stage I adenocarcinoma of the lung. *Ann Surg Oncol.* 2015;22: 4089–4097.
5. Kodama K, Higashiyama M, Yokouchi H, et al. Prognostic value of ground-glass opacity found in small lung adenocarcinoma on high-resolution CT scanning. *Lung Cancer.* 2001;33:17–25.
6. Suzuki K, Kusumoto M, Watanabe S, et al. Radiologic classification of small adenocarcinoma of the lung: radiologic-pathologic correlation and its prognostic impact. *Ann Thorac Surg.* 2006;81: 413–419.
7. Shiono S, Abiko M, Sato T. Positron emission tomography/computed tomography and lymphovascular invasion predict recurrence in stage I lung cancers. *J Thorac Oncol.* 2011;6:43–47.
8. Kim HR, Kim DJ, Lee WW, et al. The significance of maximum standardized uptake values in patients with stage I pulmonary adenocarcinoma. *Eur J Cardiothorac Surg.* 2009;35:712–716.
9. Okada M, Nakayama H, Okumura S, et al. Multicenter analysis of high-resolution computed tomography and positron emission tomography/computed tomography findings to choose therapeutic strategies for clinical stage IA lung adenocarcinoma. *J Thorac Cardiovasc Surg.* 2011;141:1384–1391.
10. Goldstraw P. The 7th edition of TNM in lung cancer: what now? *J Thorac Oncol.* 2009;4:671–673.
11. Rusch VW, Asamura H, Watanabe H, et al. The IASLC lung cancer staging project: a proposal for a new international lymph node map in the forthcoming seventh edition of the TNM classification for lung cancer. *J Thorac Oncol.* 2009;4:568–577.
12. Choi CM, Kim MY, Hwang HJ, et al. Advanced adenocarcinoma of the lung: comparison of CT characteristics of patients with anaplastic lymphoma kinase gene rearrangement and those with epidermal growth factor receptor mutation. *Radiology.* 2015;275:272–279.
13. Strauss GM, Herndon JE II, Maddaus MA, et al. Adjuvant paclitaxel plus carboplatin compared with observation in stage IB non-small-cell lung cancer: CALGB 9633 with the Cancer and Leukemia Group B, Radiation Therapy Oncology Group, and North Central Cancer Treatment Group Study Groups. *J Clin Oncol.* 2008;26:5043–5051.
14. Noguchi M. Stepwise progression of pulmonary adenocarcinoma—clinical and molecular implications. *Cancer Metastasis Rev.* 2010;29:15–21.
15. Min JH, Lee HY, Lee KS, et al. Stepwise evolution from a focal pure pulmonary ground-glass opacity nodule into an invasive lung adenocarcinoma: an observation for more than 10 years. *Lung Cancer.* 2010;69:123–126.
16. Takashima S, Maruyama Y, Hasegawa M, et al. CT findings and progression of small peripheral lung neoplasms having a replacement growth pattern. *AJR Am J Roentgenol.* 2003;180:817–826.
17. Lederlin M, Puderbach M, Muley T, et al. Correlation of radio- and histomorphological pattern of pulmonary adenocarcinoma. *Eur Respir J.* 2013;41:943–951.
18. Zerhouni EA, Stitik FP, Siegelman SS, et al. CT of the pulmonary nodule: a cooperative study. *Radiology.* 1986;160:319–327.
19. Choi CM, Kim MY, Lee JC, et al. Advanced lung adenocarcinoma harboring a mutation of the epidermal growth factor receptor: CT findings after tyrosine kinase inhibitor therapy. *Radiology.* 2014;270:574–582.
20. Sim HJ, Choi SH, Chae EJ, et al. Surgical management of pulmonary adenocarcinoma presenting as a pure ground-glass nodule. *Eur J Cardiothorac Surg.* 2014;46:632–636.
21. Chae HD, Park CM, Park SJ, et al. Computerized texture analysis of persistent part-solid ground-glass nodules: differentiation of preinvasive lesions from invasive pulmonary adenocarcinomas. *Radiology.* 2014;273:285–293.
22. Song YS, Park CM, Park SJ, et al. Volume and mass doubling times of persistent pulmonary subsolid nodules detected in patients without known malignancy. *Radiology.* 2014;273:276–284.